文章编号:1672-6553-2024-22(4)-023-007
DOI:10.6052/1672-6553-2023-119

复合材料点阵夹芯板非线性组合共振特性研究*

马婷[1] 张伟[2†]

(1. 北京工业大学 材料与制造学部,北京 100124)

(2. 广西大学 土木建筑工程学院,南宁 530004)

摘要 复合材料点阵夹芯板在 1:3 内共振和外部组合共振同时发生时的非线性共振问题被研究. 首先,基于哈密顿原理和分层位移场理论建立了复合材料夹芯板的振动偏微分方程,然后利用多尺度方法求解了伽辽金离散后的常微分方程,并得到了内共振和组合共振同时存在下夹芯板的协调方程. 最后利用数值方法得到了协调方程稳态平衡解随系统参数变化的分岔图. 研究了不同点阵芯子胞元构型,外激励频率以及外激励幅值对复合材料点阵夹芯板非线性组合共振特性所产生的影响.

关键词 夹芯板, 组合共振, 点阵, 非线性, 内共振

中图分类号:O322 **文献标志码**:A

Research on Nonlinear Combination Resonance Characteristics of Composite Lattice Sandwich Piate*

Ma Ting[1] Zhang Wei[2†]

(1. College of Mechanical Engineering, Beijing University of Technology, Beijing 100124, China)

(2. School of Civil Engineering and Architecture, Guangxi University, Nanning 530004, China)

Abstract The nonlinear resonance problem of composite lattice sandwich panels is studied when both 1:3 internal resonance and external combined resonance occur simultaneously. Firstly, based on Hamiltonian principle and layered displacement field theory, the vibration partial differential equation of composite sandwich panels was established. Then, the ordinary differential equation obtained by Galerkin discretization was solved using multi-scale method, and the modulation equation of the sandwich panel was obtained in the presence of both internal and combination resonances. Finally, the bifurcation diagram of the steady-state equilibrium solution of the modulation equation with changes in system parameters was obtained using numerical methods. The effects of different lattice core cell configurations, external excitation frequencies, and external excitation amplitudes on the nonlinear combined resonance characteristics of composite lattice sandwich panels is studied.

Key words sandwich panel, combination resonance, lattice, nonlinear, internal resonance

引言

复合材料夹层结构是由三层以上的材料或者结构组成的复合结构,有两层面板结构,其间夹着一层厚而轻的芯材,芯材维持了两面板之间的距离,使夹层面板截面的惯性矩和弯曲刚度增大. 大

2023-11-07 收到第 1 稿,2023-11-23 收到修改稿.

* 国家自然科学基金资助项目(11832002,12072201),National Natural Science Foundation of China(11832002,12072201).

† 通信作者 E-mail:sandyzhang9@163.com

大减轻结构的自重.复合材料夹层板结构以其刚度大,质量轻及良好的抗冲性能、隔声性能而备受关注,已被用于汽车、桥梁、医疗、飞行器、高速列车、船舶及潜艇等领域.此外,工程结构经常出现结构振动问题,这会加速夹层结构的失效.因此,有必要对夹层结构的动力特性进行研究.

近几年,对夹层结构动力学与静力学特性的研究吸引了许多学者的注意.Guo等[1]提出了一种有效的方法来研究金字塔点阵夹层板的自由振动问题.Lou等[2]研究了点阵夹层梁在几种典型边界条件下的自由振动问题.Hao等[3]报道了功能梯度材料夹层双曲扁壳在平面内激励下的稳定性,并计算了分叉阈值和结构在热环境中的稳定性.Kao等[4]研究了具有刚性复合材料上下面板并被泡沫填充的夹芯板在任意周期载荷作用下的动态稳定性.Chen等[5]研究了具有碳纤维增强复合材料金字塔点阵夹芯板的非线性振动特性.Yao和Li[6]研究了具有粘弹性表面的金字塔点阵夹层板在简谐外激励下的非线性主共振特性.Qin等[7]研究了具有横向可压缩芯子的几何非线性夹层梁在组合内共振情况下模态的相互作用行为.刘金辉等[8]将薄膜型声学超材料结构与格栅夹层板结构相结合,发展了一种双层薄膜型超材料夹层板结构.朱绍涛等[9]研究了负泊松比蜂窝夹层板非线性动力系统的多周期解分岔问题.Settet等[10]分析了具有磁流变弹性体芯的夹层结构在永磁场作用下的非线性磁力学行为.

鉴于以上文献的分析,对复合材料点阵夹芯板非线性共振特性的研究还是很有限的.尤其对主共振以外的次共振特性更为罕见.本研究的新颖性是研究了组合共振与内共振同时存在时复合材料点阵夹芯板的高维非线性动力学特性.基于分层位移场理论和冯卡门大变形关系,通过哈密顿原理建立了复合材料点阵夹芯板的动力学模型,研究了夹芯板的结构参数和外部激励参数对夹芯板非线性共振系统特性的影响.

1 基本方程

复合材料点阵夹芯板如图1所示,上下复合材料面板层的厚度为 h_f,芯子层厚度为 h_c,总厚度为 h,长和宽分别为 a 和 b,夹层结构受到横向均匀的简谐激励 $F(x,y,t)=q_0\cos(\Omega_1 t)$.其中 q_0 为激励幅值,Ω_1 是外激励频率.

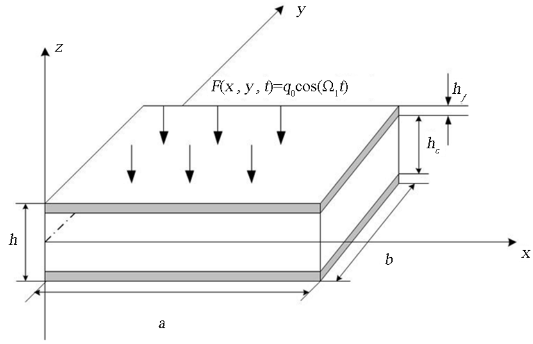

图1 复合材料点阵夹芯板示意图

Fig. 1 Schematic diagram of composite material lattice sandwich plate

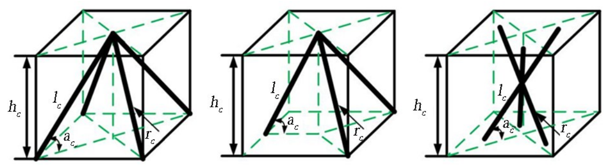

图2 不同构型芯子胞元示意图

Fig. 2 Schematic diagram of core cells with different configurations

图2为点阵芯子层的胞元构型,从左到右依次为金字塔胞元,四面体胞元和Kagome胞元.

根据受力变形后的几何关系可以得到金字塔、Kagome和四面体胞元芯子层的等效剪切模量分别为[11]:

$$G_p=\frac{\rho_1}{8}E_l\sin^2 2\alpha_c,\quad G_t=\frac{\rho_2}{8}E_l\sin^2 2\alpha_c,$$
$$G_k=\frac{\rho_3}{8}E_l\sin^2 2\alpha_c \tag{1}$$

其中 E_l 为芯杆材料弹性模量,为了方便书写芯子层剪切模量将统一表示为 G_c.

复合材料点阵夹芯板的位移场为:

$$u^{(u)}=u_0-\frac{h_c}{2}\theta_x-\left(z-\frac{h_c}{2}\right)\frac{\partial w}{\partial x},$$
$$v^{(u)}=v_0-\frac{h_c}{2}\theta_y-\left(z-\frac{h_c}{2}\right)\frac{\partial w}{\partial y},\ w^{(u)}=w_0 \tag{2a}$$

$$u^{(l)}=u_0+\frac{h_c}{2}\theta_x-\left(z+\frac{h_c}{2}\right)\frac{\partial w}{\partial x},$$
$$v^{(l)}=v_0+\frac{h_c}{2}\theta_y-\left(z+\frac{h_c}{2}\right)\frac{\partial w}{\partial y},\ w^{(l)}=w_0 \tag{2b}$$

$$u^{(c)}=u_0-z\theta_x,\ v^{(c)}=v_0-z\theta_y,\ w^{(c)}=w_0 \tag{2c}$$

其中 (u_0,v_0,w_0) 为中面位移,θ_x 和 θ_y 为中面转角.角标 u 和 l 代表上下面板,角标 c 代表芯子层.

根据冯卡门几何大变形关系,我们可以得到上

下复合材料面板以及芯子层的非线性位移应变关系为:

$$\boldsymbol{\varepsilon}^{(\alpha)}=\boldsymbol{\varepsilon}_0^{(\alpha)}+z\boldsymbol{\kappa}\ ,\boldsymbol{\varepsilon}^{(c)}=\boldsymbol{\gamma}\ ,(\alpha=u,l) \tag{3}$$

其中

$$\boldsymbol{\varepsilon}^{(\alpha)}=\begin{pmatrix}\varepsilon_{xx}^{(\alpha)}\\ \varepsilon_{yy}^{(\alpha)}\\ \gamma_{xy}^{(\alpha)}\end{pmatrix},\boldsymbol{\varepsilon}_0^{(\alpha)}=\begin{pmatrix}\varepsilon_{xx0}^{(\alpha)}\\ \varepsilon_{yy0}^{(\alpha)}\\ \gamma_{xy0}^{(\alpha)}\end{pmatrix},$$

$$\boldsymbol{\kappa}=\begin{pmatrix}\varepsilon_{xx1}^{(\alpha)}\\ \varepsilon_{yy1}^{(\alpha)}\\ \gamma_{xy1}^{(\alpha)}\end{pmatrix},(\alpha=u,l),\boldsymbol{\gamma}=\begin{pmatrix}\gamma_{yz}^{(c)}\\ \gamma_{xz}^{(c)}\end{pmatrix} \tag{4}$$

公式(4)中矩阵向量的具体形式可以参见文献[8].

上下复合材料面板第 k 层本构关系为:

$$(\boldsymbol{\sigma}^{(\alpha)})^k=\bar{\boldsymbol{Q}}(\boldsymbol{\varepsilon}^{(\alpha)}),\bar{\boldsymbol{Q}}=\boldsymbol{T}_k^{-1}\boldsymbol{Q}(\boldsymbol{T}_k^{-1})^{\mathrm{T}} \tag{5a}$$

展开式为:

$$\boldsymbol{\sigma}^{(\alpha)}=\begin{pmatrix}\sigma_{xx}^{(\alpha)}\\ \sigma_{yy}^{(\alpha)}\\ \sigma_{xy}^{(\alpha)}\end{pmatrix},\boldsymbol{\varepsilon}^{(\alpha)}=\begin{pmatrix}\varepsilon_{xx}^{(\alpha)}\\ \varepsilon_{yy}^{(\alpha)}\\ \gamma_{xy}^{(\alpha)}\end{pmatrix},(\alpha=u,l) \tag{5b}$$

其中刚度矩阵 $\boldsymbol{Q}$ 和坐标转换矩阵 $\boldsymbol{T}_k$ 分别为

$$\boldsymbol{Q}=\begin{bmatrix}Q_{11}&Q_{12}&0\\ Q_{12}&Q_{22}&0\\ 0&0&Q_{66}\end{bmatrix},$$

$$\boldsymbol{T}_k=\begin{bmatrix}\cos^2\theta&\sin^2\theta&2\sin\theta\cos\theta\\ \sin^2\theta&\cos^2\theta&-2\sin\theta\cos\theta\\ -\sin\theta\cos\theta&\sin\theta\cos\theta&\cos^2\theta-\sin^2\theta\end{bmatrix} \tag{6}$$

其中

$$Q_{11}=\frac{E_1}{1-v_{12}v_{21}},Q_{12}=\frac{v_{12}E_2}{1-v_{12}v_{21}},$$

$$Q_{22}=\frac{E_2}{1-v_{12}v_{21}},Q_{66}=G_{12} \tag{7}$$

只考虑芯子层的剪切变形,则其本构方程为:

$$\begin{bmatrix}\tau_{yz}^{(c)}\\ \tau_{xz}^{(c)}\end{bmatrix}=\begin{bmatrix}G_c&0\\ 0&G_c\end{bmatrix}\begin{bmatrix}\gamma_{yz}^{(c)}\\ \gamma_{xz}^{(c)}\end{bmatrix} \tag{8}$$

基于哈密顿原理,得到复合材料点阵夹芯板振动偏微分方程为:

$$\frac{\partial}{\partial x}(N_{xx}^u+N_{xx}^l)+\frac{\partial}{\partial y}(N_{xy}^u+N_{xy}^l)=(2I_0^{\rho_f}+I_0^{\rho_c})\ddot{u}_0-I_1^{\rho_c}\ddot{\theta}_x \tag{9a}$$

$$\frac{\partial}{\partial y}(N_{yy}^u+N_{yy}^l)+\frac{\partial}{\partial x}(N_{xy}^u+N_{xy}^l)=(2I_0^{\rho_f}+I_0^{\rho_c})\ddot{v}_0-I_1^{\rho_c}\ddot{\theta}_y \tag{9b}$$

$$\begin{aligned}&\frac{\partial}{\partial x}\left[(N_{xx}^u+N_{xx}^l)\frac{\partial w_0}{\partial x}\right]+\frac{\partial}{\partial y}\left[(N_{yy}^u+N_{yy}^l)\frac{\partial w_0}{\partial y}\right]+\\&\frac{\partial}{\partial y}\left[(N_{xy}^u+N_{xy}^l)\frac{\partial w_0}{\partial x}\right]+\frac{\partial}{\partial x}\left[(N_{xy}^u+N_{xy}^l)\frac{\partial w_0}{\partial y}\right]+\\&\frac{\partial^2}{\partial x^2}(M_{xx}^u+M_{xx}^l)-\frac{h_c}{2}\frac{\partial^2}{\partial y^2}(N_{yy}^u-N_{yy}^l)+\frac{\partial Q_x^{(c)}}{\partial x}+\\&\frac{\partial^2}{\partial y^2}(M_{yy}^u+M_{yy}^l)-\frac{h_c}{2}\frac{\partial^2}{\partial x^2}(N_{xx}^u-N_{xx}^l)+\frac{\partial Q_y^{(c)}}{\partial y}+\\&2\frac{\partial^2}{\partial x\partial y}(M_{xy}^u+M_{xy}^l)-h_c\frac{\partial^2}{\partial x\partial y}(N_{xy}^u-N_{xy}^l)+F-\\&\gamma\dot{w}_0=-\left[h_cI_1^{\rho_f}-\frac{h_c^2}{2}I_0^{\rho_f}\right]\left(\frac{\partial\theta_x}{\partial x}+\frac{\partial\ddot{\theta}_x}{\partial x}\right)+(2I_0^{\rho_f}+\\&I_0^{\rho_c})\ddot{w}_0-\left[2(I_2^{\rho_f})-2h_c(I_1^{\rho_f})+\frac{h_c^2}{2}(I_0^{\rho_f})\right]\times\\&\left(\frac{\partial^2\ddot{w}_0}{\partial x^2}+\frac{\partial^2\ddot{w}_0}{\partial y^2}\right)\end{aligned} \tag{9c}$$

$$\begin{aligned}&-\frac{h_c}{2}\frac{\partial}{\partial x}(N_{xx}^u-N_{xx}^l)-\frac{h_c}{2}\frac{\partial}{\partial y}(N_{xy}^u-N_{xy}^l)+Q_x^{(c)}\\&=\left[\frac{h_c^2}{2}(I_0^{\rho_f})+I_2^{\rho_c}\right]\ddot{\theta}_x+\\&\left[h_c(I_1^{\rho_f})-\frac{h_c^2}{2}(I_0^{\rho_f})\right]\frac{\partial\ddot{w}_0}{\partial x}-I_1^{\rho_c}\ddot{u}_0\end{aligned} \tag{9d}$$

$$\begin{aligned}&-\frac{h_c}{2}\frac{\partial}{\partial y}(N_{yy}^u-N_{yy}^l)-\frac{h_c}{2}\frac{\partial}{\partial x}(N_{xy}^u-N_{xy}^l)+Q_y^{(c)}\\&=\left[\frac{h_c^2}{2}(I_0^{\rho_f})+I_2^{\rho_c}\right]\ddot{\theta}_y+\\&\left[h_c(I_1^{\rho_f})-\frac{h_c^2}{2}(I_0^{\rho_f})\right]\frac{\partial\ddot{w}_0}{\partial y}-I_1^{\rho_c}\ddot{v}_0\end{aligned} \tag{9e}$$

其中

$$\begin{aligned}\begin{pmatrix}N_{xx}^{(\alpha)}\\ N_{yy}^{(\alpha)}\\ N_{xy}^{(\alpha)}\end{pmatrix}&=\begin{bmatrix}A_{11}^{\alpha}&A_{12}^{\alpha}&A_{16}^{\alpha}\\ A_{12}^{\alpha}&A_{22}^{\alpha}&A_{26}^{\alpha}\\ A_{16}^{\alpha}&A_{26}^{\alpha}&A_{66}^{\alpha}\end{bmatrix}\begin{pmatrix}\varepsilon_{xx0}^{(\alpha)}\\ \varepsilon_{yy0}^{(\alpha)}\\ \gamma_{xy0}^{(\alpha)}\end{pmatrix}+\\&\begin{bmatrix}B_{11}^{\alpha}&B_{12}^{\alpha}&B_{16}^{\alpha}\\ B_{12}^{\alpha}&B_{22}^{\alpha}&B_{26}^{\alpha}\\ B_{16}^{\alpha}&B_{26}^{\alpha}&B_{66}^{\alpha}\end{bmatrix}\begin{pmatrix}\varepsilon_{xx1}^{(\alpha)}\\ \varepsilon_{yy1}^{(\alpha)}\\ \gamma_{xy1}^{(\alpha)}\end{pmatrix}\end{aligned} \tag{10a}$$

$$\begin{aligned}\begin{pmatrix}M_{xx}^{(\alpha)}\\ M_{yy}^{(\alpha)}\\ M_{xy}^{(\alpha)}\end{pmatrix}&=\begin{bmatrix}B_{11}^{\alpha}&B_{12}^{\alpha}&B_{16}^{\alpha}\\ B_{12}^{\alpha}&B_{22}^{\alpha}&B_{26}^{\alpha}\\ B_{16}^{\alpha}&B_{26}^{\alpha}&B_{66}^{\alpha}\end{bmatrix}\begin{pmatrix}\varepsilon_{xx0}^{(\alpha)}\\ \varepsilon_{yy0}^{(\alpha)}\\ \gamma_{xy0}^{(\alpha)}\end{pmatrix}+\\&\begin{bmatrix}D_{11}^{\alpha}&D_{12}^{\alpha}&D_{16}^{\alpha}\\ D_{12}^{\alpha}&D_{22}^{\alpha}&D_{26}^{\alpha}\\ D_{16}^{\alpha}&D_{26}^{\alpha}&D_{66}^{\alpha}\end{bmatrix}\begin{pmatrix}\varepsilon_{xx1}^{(\alpha)}\\ \varepsilon_{yy1}^{(\alpha)}\\ \gamma_{xy1}^{(\alpha)}\end{pmatrix}\end{aligned} \tag{10b}$$

$$\begin{bmatrix} Q_y^{(c)} \\ Q_x^{(c)} \end{bmatrix} = \begin{bmatrix} A_{44}^{(c)} & 0 \\ 0 & A_{55}^{(c)} \end{bmatrix} \begin{bmatrix} \gamma_{yz}^{(c)} \\ \gamma_{xz}^{(c)} \end{bmatrix}, (\alpha = u, l) \tag{10c}$$

$$A_{ii}^{(c)} = \int_{-\frac{h_c}{2}}^{\frac{h_c}{2}} G_c \mathrm{d}z. \quad (i = 4, 5) \tag{10d}$$

$$(I_0^{\rho_c} \quad I_1^{\rho_c} \quad I_2^{\rho_c}) = \int_{-\frac{h_c}{2}}^{\frac{h_c}{2}} \rho_c (1, \quad z, \quad z^2) \mathrm{d}z \tag{10e}$$

$$(I_0^{\rho_f} \quad I_1^{\rho_f} \quad I_2^{\rho_f}) = \int_{z_{u(1)}}^{z_{u(n+1)}} \rho_f (1, \quad z, \quad z^2) \mathrm{d}z \tag{10f}$$

$$(A_{ij}^l \quad B_{ij}^l \quad D_{ij}^l) = \sum_{k=1}^{n} \int_{z_{l(k)}}^{z_{l(k+1)}} (\bar{Q}_{ij})_k (1, \quad z, \quad z^2) \mathrm{d}z \tag{10g}$$

$$(A_{ij}^u \quad B_{ij}^u \quad D_{ij}^u) = \sum_{k=1}^{n} \int_{z_{u(k)}}^{z_{u(k+1)}} (\bar{Q}_{ij})_k (1, \quad z, \quad z^2) \mathrm{d}z \quad (i, j = 1, 2, 6) \tag{10h}$$

其中 ρ_f 为上下面板密度，ρ_c 为芯子的等效密度. 积分上下限分别为上下复合材料面板每层顶部和底部距离中性面的距离. $(N_{xx}^{(\alpha)} \quad N_{yy}^{(\alpha)} \quad N_{xy}^{(\alpha)})$ 为夹芯板上下面板每单位长度上面内合力，$(M_{xx}^{(\alpha)} \quad M_{yy}^{(\alpha)} \quad M_{xy}^{(\alpha)})$ 为每单位长度上合力矩，$(Q_y^{(c)} \quad Q_x^{(c)})$ 为芯子层横向合力，$(I_0^{\rho_c} \quad I_2^{\rho_f})$ 为夹芯板芯子层和上线面板的单位长度上的质量惯性矩.

基于四边简支边界条件下复合材料点阵夹芯板的线性模态分析，模态(1.1)和(3.1)两阶模态存在 1:3 内共振关系，进而选取这两阶模态将点阵夹芯板振动方程(9)进行伽辽金截断，得到复合材料点阵夹芯板的非线性振动常微分方程：

$$\ddot{w}_1 + \omega_1^2 w_1 + c_1 \gamma \dot{w}_1 + \beta_{11} w_1^3 + \beta_{12} w_1^2 w_2 + \beta_{13} w_2^2 w_1 + \beta_{14} w_2^3 = \beta_{17} q_0 \cos(\Omega_1 t) \tag{11a}$$

$$\ddot{w}_2 + \omega_2^2 w_2 + c_2 \gamma \dot{w}_2 + \beta_{21} w_1^3 + \beta_{22} w_1^2 w_2 + \beta_{23} w_2^2 w_1 + \beta_{24} w_2^3 = \beta_{27} q_0 \cos(\Omega_1 t) \tag{11b}$$

其中 c_i 和 β_{ij} $(i = 1, 2, \quad j = 1, 2, 3, 4, 7)$ 是伽辽金截断后的系数值.

引入如下参数变换：

$$\bar{w}_1 = \frac{w_1}{h}, \bar{w}_2 = \frac{w_2}{h}, \bar{t} = t\omega_1, \bar{\omega}_i^2 = \frac{\omega_i^2}{\omega_1^2},$$

$$(i = 1, 2), \bar{c}_i = \frac{c_i}{\omega_1}, (i = 1, 2), \bar{\Omega}_1 = \frac{\Omega_1}{\omega_1},$$

$$\bar{\beta}_{17} = \beta_{17} \frac{1}{\omega_1^2 h}, \bar{\beta}_{27} = \beta_{27} \frac{1}{\omega_1^2 h},$$

$$\bar{\beta}_{ij} = \beta_{ij} \frac{h^2}{\omega_1^2}, (i = 1, 2, \; j = 1, 2, 3, 4) \tag{12}$$

得到无量纲化后的振动微分方程：

$$\ddot{\bar{w}}_1 + \bar{\omega}_1^2 \bar{w}_1 + \bar{c}_1 \gamma \dot{\bar{w}}_1 + \bar{\beta}_{11} \bar{w}_1^3 + \bar{\beta}_{12} \bar{w}_1^2 \bar{w}_2 + \bar{\beta}_{13} \bar{w}_2^2 \bar{w}_1 + \bar{\beta}_{14} \bar{w}_2^3 = \bar{\beta}_{17} q_0 \cos(\Omega_1 t) \tag{13a}$$

$$\ddot{\bar{w}}_2 + \bar{\omega}_2^2 \bar{w}_2 + \bar{c}_2 \gamma \dot{\bar{w}}_2 + \bar{\beta}_{21} \bar{w}_1^3 + \bar{\beta}_{22} \bar{w}_1^2 \bar{w}_2 + \bar{\beta}_{23} \bar{w}_2^2 \bar{w}_1 + \bar{\beta}_{24} \bar{w}_2^3 = \bar{\beta}_{27} q_0 \cos(\Omega_1 t) \tag{13b}$$

为了方便后续书写，字母上方的横线将被省略掉.

运用多尺度方法求解点阵夹芯板非线性振动方程. 首先引进快慢时间尺度 $T_0 = t$ 和 $T_1 = \varepsilon t$，对时间的一阶和二阶导数变为：

$$\frac{\mathrm{d}}{\mathrm{d}t} = \frac{\partial}{\partial T_0} \frac{\partial T_0}{\partial t} + \frac{\partial}{\partial T_1} \frac{\partial T_1}{\partial t} + \cdots = D_0 + \varepsilon D_1 + \cdots \tag{14a}$$

$$\frac{\mathrm{d}^2}{\mathrm{d}t^2} = (D_0{}^2 + 2\varepsilon D_0 D_1 + \cdots) \tag{14b}$$

其中 $D_n = \frac{\partial}{\partial t_n}$.

引入如下尺度变换：

$$c_i = \varepsilon c_i, \beta_{ij} = \varepsilon \beta_{ij}, (i = 1, 2, \quad j = 1, 2, 3, 4) \tag{15}$$

则原非线性振动方程变为：

$$\ddot{w}_1 + \omega_1^2 w_1 + \varepsilon c_1 \gamma \dot{w}_1 + \varepsilon \beta_{11} w_1^3 + \varepsilon \beta_{12} w_1^2 w_2 + \varepsilon \beta_{13} w_2^2 w_1 + \varepsilon \beta_{14} w_2 = \beta_{17} q_0 \cos(\Omega_1 t) \tag{16a}$$

$$\ddot{w}_2 + \omega_2^2 w_2 + \varepsilon c_2 \gamma \dot{w}_2 + \varepsilon \beta_{21} w_1^3 + \varepsilon \beta_{22} w_1^2 w_2 + \varepsilon \beta_{23} w_2^2 w_1 + \varepsilon \beta_{24} w_2^3 = \beta_{27} q_0 \cos(\Omega_1 t) \tag{16b}$$

然后将方程的解展开为的幂级数形式：

$$w_1 = w_{10}(T_0, T_1) + \varepsilon w_{11}(T_0, T_1) \tag{17a}$$

$$w_2 = w_{20}(T_0, T_1) + \varepsilon w_{21}(T_0, T_1) \tag{17b}$$

将方程(17)代入到方程(16)中，然后令等式两边的同次幂项的系数相等，得到如下形式的微分方程：

Order ε^0：

$$D_0^2 w_{i0} + \omega_i^2 w_{i0} = \beta_{i7} q_0 \cos(\Omega_1 t), (i = 1, 2) \tag{18}$$

Order ε^1：

$$D_0^2 w_{11} + \omega_1^2 w_{11} = -2D_0 D_1 w_{10} - c_1 \gamma D_0 w_{10} - \beta_{11} w_{10}^3 - \beta_{12} w_{10}^2 w_{20} - \beta_{13} w_{10} w_{20}^2 - \beta_{14} w_{20}^3 \tag{19a}$$

$$D_0^2 w_{21} + \omega_2^2 w_{21} = -2D_0 D_1 w_{20} - c_2 \gamma D_0 w_{20} - \beta_{21} w_{10}^3 - \beta_{22} w_{10}^2 w_{20} - \beta_{23} w_{10} w_{20}^2 - \beta_{24} w_{20}^3 \tag{19b}$$

方程(18)的解为:

$$w_{10}=A_1(T_1)e^{i\omega_{10}T_0}+\bar{A}_1(T_1)e^{-i\omega_{10}T_0}+A_3e^{i\Omega_1T_0}+\bar{A}_3e^{-i\Omega_1T_0}$$

$$w_{20}=A_2(T_1)e^{i\omega_{20}T_0}+\bar{A}_2(T_1)e^{-i\omega_{20}T_0}+A_4e^{i\Omega_1T_0}+\bar{A}_4e^{-i\Omega_1T_0} \tag{20}$$

其中 $A_3=\dfrac{\beta_{17}q_0}{2(\omega_{10}{}^2-\Omega_1)}$, $A_3=\dfrac{\beta_{17}q_0}{2(\omega_{10}{}^2-\Omega_1)}$, $\bar{A}_i(i=1,2,3,4)$ 表示 A_i 的复数共轭.

本文研究点阵夹芯板在内共振和组合共振同时存在情况下的共振特性,引入调谐参数 $\sigma_i(i=1,2)$,共振关系可以表示为:

$$\Omega_1=\omega_{20}+2\omega_{10}+\varepsilon\sigma_1,\ \omega_{20}=3\omega_{10}+\varepsilon\sigma_2 \tag{21}$$

引入极坐标变换

$$A_j=\frac{1}{2}a_je^{i\beta_j}\ (j=1,2) \tag{22}$$

其中 a_j 和 β_j 是 T_1 的实值函数.

我们可以得到点阵夹芯板组合共振情况下的协调方程详细推导过程见文献[12]:

$$8\omega_1\dot{a}_1=-4\omega_1c_1\gamma a_1-\beta_{12}a_1^2a_2\sin\varphi_2 \tag{23a}$$

$$8\omega_1a_1\dot{\beta}_1=\beta_{12}a_2a_1{}^2+3\beta_{11}a_1^3+2\beta_{13}a_1a_2^2+16\beta_{12}A_3\bar{A}_4a_1+24\beta_{11}A_3^2a_1+8\beta_{13}A_4\bar{A}_4a_1 \tag{23b}$$

$$8\omega_2\dot{a}_2=-4c_2\gamma\omega_2a_2-6\beta_{24}A_4a_2^2\sin\varphi_1-2\beta_{23}A_3a_2^2\sin\varphi_1+\beta_{21}a_1^3\sin\varphi_2 \tag{23c}$$

$$8\omega_2a_2\dot{\beta}_2=\beta_{21}a_1^3\cos\varphi_2+2\beta_{23}A_3a_2^2\cos\varphi_1+2\beta_{22}a_1^2a_2+6\beta_{24}A_4a_2^2\cos\varphi_1+3\beta_{24}a_2^3+16\beta_{23}A_3\bar{A}_4a_2+8\beta_{22}A_3^2a_2+24\beta_{24}A_4^2a_2 \tag{23d}$$

其中 $\varphi_1=\sigma_1T_1-3\beta_2,\varphi_2=\sigma_2T_1-3\beta_1+\beta_2$.

2　数值模拟

图 3 为复合材料点阵夹芯板发生组合共振情况下两个模态的幅频响应曲线,其中图 3(a)为金字塔胞元构型夹芯板的幅频曲线,图 3(b)为 Kagome 胞元夹芯板的幅频响应曲线,图 3(c)为四面体胞元夹芯板幅频响应曲线,图 3(d)为不同芯子胞元构型夹芯板的第一阶模态的幅频曲线,图 3(e)为不同芯子胞元构型夹芯板的第二阶模态的幅频曲线.

由图可知,两阶模态展现出来的特性之所以会不同是因为不同于线性振动,非线性共振发生时,由于特定的外激频率与夹芯板固有频率的倍数关系,导致了不同的非线性项以及结构参数值进入了影响模态幅值的协调方程中,数值计算后,得到非线性两阶模态幅值变化趋势就会展现出线性系统不存在的非线性特有的共振特性.

夹芯板组合共振幅频曲线在激励频率较小时,不存在实数解,即当激励频率较小时,组合共振不会发生.随着激励频率的增加,三种芯子单胞夹芯板的两个模态的稳定解支的幅值均呈现单调增大

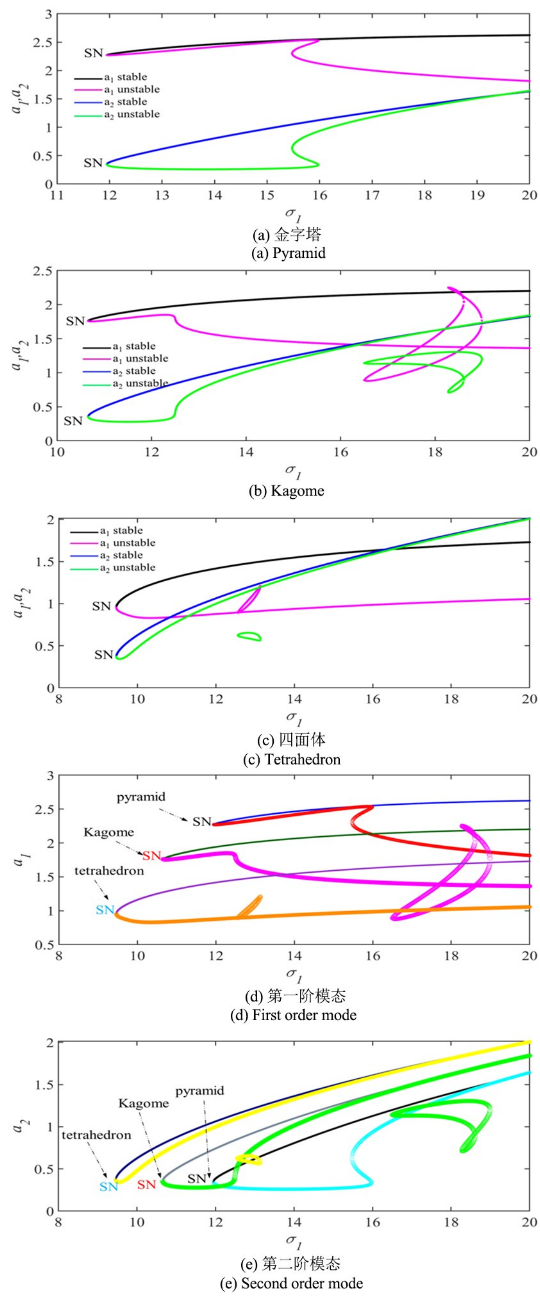

(a) 金字塔
(a) Pyramid
(b) Kagome
(c) 四面体
(c) Tetrahedron
(d) 第一阶模态
(d) First order mode
(e) 第二阶模态
(e) Second order mode

图 3　不同芯子单胞构型夹芯板组合共振幅频曲线

Fig. 3　Amplitude frequency curves of sandwich panels with different core unit cell configurations under combination resonance conditions

的趋势. 相对于金字塔单胞夹芯板，四面体和 Kagome 胞元夹芯板的幅频响应多了一对不稳定的封闭形式的两解曲线. 不用胞元构型夹芯板第一阶模态的稳定解支按照由大到小的顺序分别是金字塔单胞、Kagome 单胞和四面体单胞，而不同胞元构型夹芯板的第二阶模态的稳定解支的大小顺序则与第一阶模态的顺序恰好相反.

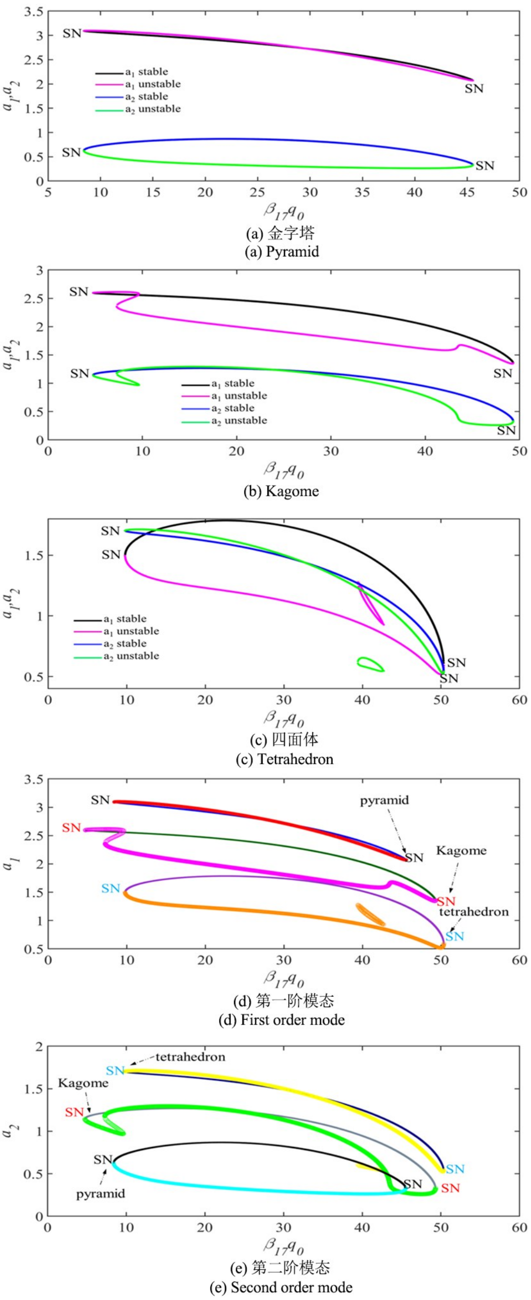

图 4 不同芯子单胞构型夹芯板组合共振力幅曲线

Fig. 4 Force amplitude curves of sandwich panels with different core unit cell configurations under combination resonance conditions

图 4 为复合材料点阵夹芯板发生组合共振情况下两个模态的力幅响应曲线，其中图 4(a) 为金字塔胞元构型夹芯板的力幅曲线，图 4(b) 为 Kagome 胞元夹芯板的力幅响应曲线，图 4(c) 为四面体胞元夹芯板力幅响应曲线，图 4(d) 为不同芯子胞元构型夹芯板的第一阶模态的力幅曲线，图 4(e) 为不同芯子胞元构型夹芯板的第二阶模态的力幅曲线.

由图可知，夹芯板力幅曲线在激励幅值较大或者较小时均不存在实数解，所以得出夹芯板只有在特定的横向激励幅值范围内才会发生非线性组合共振. 随着激励幅值的增加，金字塔胞元夹芯板第一阶模态稳定振幅值单调减少，第二阶模态则先缓慢增加然后呈现减少的趋势. Kagome 胞元夹芯板的两个模态的稳定解支变化趋势与金字塔相同. 四面体胞元夹芯板的第一阶模态的稳定解支随着激励幅值的增加呈现先增大后减少的趋势，第二阶模态则是随着激励幅值的增加一直单调减少. 四面体胞元夹芯板力幅曲线相对于金字塔和 Kagome 夹芯板多了一对不稳定的两解封闭曲线. 不用胞元构型夹芯板第一阶模态力幅曲线的稳定解支按照由大到小的顺序分别是金字塔单胞、Kagome 单胞和四面体单胞，而第二阶模态的稳定解支的大小顺序则与第一阶模态的顺序相反.

3 结论

本文研究了复合材料点阵夹心板的非线性动力学特性. 基于非线性几何大变形理论，运用哈密顿原理建立了夹芯板的非线性振动方程. 研究了不同芯子胞元构型对夹芯板非线性振动特性的影响. 芯子单胞构型定性的改变了夹芯板幅频曲线和力幅曲线的变化趋势，随着激励频率的增加，不同单胞夹芯板两个模态的稳定振幅值均呈现单调增加的趋势，而随着激励幅值的增加，不同胞元夹芯板两个模态的变化趋势各不相同. 综合比较三种胞元构型，四面体单胞构型的设计使夹芯板组合共振时的振幅值最小，此外减小外激励的频率可以大大减小夹芯板组合共振时的振幅值，或者将激励幅值避开共振区域的参数区间可以从根本上抑制夹芯板组合共振现象的发生. 减少结构非线性共振对工程结构的破坏.

参考文献

[1] GUO Z K, LIU C C, LI F M. Vibration analysis of

sandwich plates with lattice truss core [J]. Mechanics of Advanced Materials and Structures, 2019, 26 (5): 424－429.

[2] LOU J, WANG B, MA L, et al. Free vibration analysis of lattice sandwich beams under several typical boundary conditions [J]. Acta Mechanica Solida Sinica, 2013, 26(5): 458－467.

[3] HAO Y X, CAO Z, ZHANG W, et al. Stability analysis for geometric nonlinear functionally graded sandwich shallow shell using a new developed displacement field [J]. Composite Structures, 2019, 210: 202－216.

[4] KAO J Y, CHEN C S, CHEN W R. Parametric vibration response of foam-filled sandwich plates under periodic loads [J]. Mechanics of Composite Materials, 2012, 48: 525－538.

[5] CHEN J E, ZHANG W, SUN M, et al. Parametric study on nonlinear vibration of composite truss core sandwich plate with internal resonance [J]. Journal of Mechanical Science and Technology, 2016, 30 (9): 4133－4142.

[6] YAO G, LI F M. Nonlinear primary resonances of lattice sandwich beams with pyramidal truss core and viscoelastic surfaces [J]. Acta Mechanica, 2018, 229(10): 4091－4100.

[7] QIN Z M, FENG Y Z, ZHAO G P. Modal interactions of a geometrically nonlinear sandwich beam with transversely compressible core [J]. Thin-Walled Structures, 2013, 73: 242－251.

[8] 刘金辉，李金强，张垚，等. 双层薄膜型超材料夹层板的多带隙设计[J]. 动力学与控制学报，2023，21(7)：20－27

LIU J H, LI J Q, ZHANG Y, et al. Multi-bandgap design of double membrane-type acoustic metamaterials [J]. Journal of Dynamics and Control, 2023, 21(7): 20－27. (in Chinese)

[9] 朱绍涛，李静，张伟. 负泊松比蜂窝夹层板的多周期运动研究[J]. 动力学与控制学报，2021，19(5)：33－38.

ZHU S T, LI J, ZHANG W. Multiple periodic motions of a honeycomb [J]. Journal of Dynamics and Control, 2021, 19(5): 33－38. (in Chinese)

[10] SETTET A T, AGUIB S, NOUR A, et al. Study and analysis of the magneto-mechanical behavior of smart composite sandwich beam in elastomer[J]. Mechanika, 2019, 25(4): 320－325.

[11] CHAIY Y, LI F M, SONG Z G, Nonlinear vibrations, bifurcations and chaos of lattice sandwich composite panels on Winkler-Pasternak elastic foundations with thermal effects in supersonic airflow [J]. Meccanica, 2019, 54(7): 919－944.

[12] NAYFEH A H, BALACHANDRA D T. Applied nonlinear dynamics[M]. New York: Wiley, 1995: 461－485.